Journal of the European Ceramic Society 21 (2001) 1013–1019

www.elsevier.com/locate/jeurceramsoc

High-temperature effects in the fracture mechanical behaviour of silicon carbide liquid-phase sintered with $AlN–Y_2O_3$ additives

G. Rixecker *, I. Wiedmann, A. Rosinus, F. Aldinger

Max-Planck-Institut für Metallforschung and Institut für Nichtmetallische Anorganische Materialien der Universität Stuttgart, Pulvermetallurgisches Laboratorium, Heisenbergstraße 5, D-70569 Stuttgart, Germany

Received 14 September 2000; received in revised form 25 October 2000; accepted 12 November 2000

Abstract

It has been shown that pressureless sintering of SiC to theoretical density is possible with sintering additives from the system $AlN–Y_2O_3$. While commonly a combination of oxides is used such as $Al_2O_3–Y_2O_3$ ($–SiO_2$), the oxynitride additives offer the advantage that only a nitrogen atmosphere is required instead of a powder bed for thermochemical stabilisation at the sintering temperature. The thermal decomposition of AlN is suppressed quite effectively when a moderate nitrogen overpressure is applied, resulting in very small mass loss during densification which only depends on the oxygen content of the SiC starting powder. By varying the mass ratio of β-SiC to α-SiC and applying dedicated post-densification heat treatments, a platelet-strengthened microstructure is obtained which shows enhanced fracture toughness. The platelet formation is attributed to a solution / precipitation process with simultaneous phase transformation from β-SiC to α-SiC, followed by anisotropic grain growth of α-SiC. In the present work, recent progress in the mechanical properties of these materials is reported. By means of a simple surface treatment-annealing in air — it is possible to obtain four-point bending strengths in excess of 1 GPa in liquid phase sintered SiC. The strength retention at temperatures around 1200°C is significantly improved.

Keywords: Annealing; Liquid phase sintering; Mechanical properties; Microstructure-final; SiC; Sintering

1. Introduction

During the last decade, intense research activities have led to substantial progress in the properties of non-oxide ceramics. This has also resulted in a detailed insight into the mechanisms governing the microstructural evolution during liquid phase sintering of covalent materials. By choosing appropriate starting powders, sintering additives, and temperature programs, it has become possible to tailor materials with a dedicated spectrum of properties.[1]

Similar to Si_3N_4, SiC is a non-oxide ceramic with predominantly covalent bonding. Apart from its superior hardness, silicon carbide has a potential for further improvement of both high-temperature strength behaviour and oxidation resistance at temperatures above 1000°C. For mechanically demanding structural applications, favourable properties may be expected especially in liquid-phase sintered materials (LPS–SiC) because, compared to conventionally sintered SiC (SSiC), very homogeneous and fine-grained microstructures can be obtained due to the lower sintering temperatures and to the presence of the liquid phase.[2] If α-SiC is used as a starting powder, average grain sizes below 1 μm can be achieved in fully dense ceramics. If β-SiC powder containing a small amount of α-SiC seeds is used, platelet microstructures can be obtained showing grain sizes below 5 μm and an enhanced fracture toughness. Due to the fine grain structure, achievable strength values can be much higher than in SSiC. With an additional hot isostatic densification step after sintering, 4-point bending strengths above 800 MPa and an indentation fracture toughness (K_{Ic}^{ICL}) of about 5 $MPa\sqrt{m}$ have been achieved.[3] Like silicon nitride, LPS–SiC materials with tailored properties can be designed by thorough investigation of the correlations between properties, microstructures and preparation conditions.

From a technological point of view, sintering aids should enable full densification with low mass loss and without using a powder bed. The commonly used additive system $Al_2O_3–Y_2O_3$ ($–SiO_2$) does not fulfil the latter

* Corresponding author.
E-mail address: rixecker@aldix.mpi-stuttgart.mpg.de (G. Rixecker).

0955-2219/01/$ - see front matter
PII: S0955-2219(00)00317-4

criterion because at sintering temperatures, the formation of gaseous products of redox reactions between SiC and SiO_2 or Al_2O_3 is observed:[5]

$$SiO_2 + SiC \rightarrow 3SiO \uparrow + CO \uparrow \quad (1)$$

$$Al_2O_3 + SiC \rightarrow Al_2O \uparrow + SiO \uparrow + CO \uparrow \quad (2)$$

In order to suppress these decomposition reactions, a powder bed with a composition similar to the sample composition is required. A detailed description of experiments conducted with Al_2O_3–Y_2O_3 (–SiO_2) additives has been given earlier.[6] If the sintering atmosphere is chosen properly, Y_2O_3 does not show appreciable gas phase reactions with SiC.[7] With Y_2O_3 alone, however, the amount of liquid phase is not sufficient for full densification at temperatures below 2000°C. The suitability of AlN–Y_2O_3 as an alternative sintering aid was first demonstrated by Chia et al.[8] and investigated in detail in a doctoral thesis by Nader.[3] In the present work, which is mostly based on the doctoral thesis by Wiedmann,[4] the sintering behaviour, microstructural evolution and mechanical properties of LPS–SiC densified with AlN–Y_2O_3 additions are discussed. Full densification is achieved by pressureless sintering (0.1 MPa N_2) or by gas pressure sintering (0.2–10 MPa N_2). Due to the more efficient suppression of the thermal decomposition of AlN, using a nitrogen overpressure proves to be advantageous with regard to microstructure control. Comparative experiments in inert gas atmospheres (up to 10 MPa Ar) indicate that in addition there is an isostatic pressure contribution to densification.[3]

By changing the ratio of α-SiC to β-SiC in the starting powders, and by dedicated post-sintering heat treatments, the microstructure of LPS–SiC can be varied extensively.[2] During liquid phase sintering, a solution-precipitation process with simultaneous phase transition from β-SiC to α-SiC takes place: β-SiC grains are preferentially dissolved in the liquid phase, and α-SiC reprecipitates on pre-existing α-SiC seeds. Due to the hexagonal symmetry of α-SiC, the grain growth is anisotropic. As a result, a microstructure consisting of platelet-like grains is formed. Since the extent of steric hindrance during platelet growth is determined by the volume density of α-SiC seed crystals, the aspect ratio of SiC grains in the fully developed microstructure increases as the fraction of α-SiC decreases. The fracture toughness of the platelet microstructure is significantly enhanced and has a maximum of approximately 8 $MPa\sqrt{m}$ in high temperature measurements with crack tip temperatures of about 650–1050°C.[4]

For the LPS–SiC materials having fine-grained, equiaxed microstructures, a significant increase of the high-temperature bending strength is found in oxidising atmospheres, with peak temperatures between 1000 and 1200°C. Taking advantage of this effect, room temperature strengths greater than 1 GPa can be obtained by means of appropriate oxidising heat treatments. It is possible to correlate this strength behaviour with changes in the phase composition of the intergranular material, as observed by X-ray diffraction.

2. Experimental

Sample preparation followed a customary powder technology process chain. Appropriate mixtures of commercial powders of α-SiC (Lonza UF 15; Ibiden), β-SiC (HCST B 10), SiO_2 (Degussa Aerosil), α-Al_2O_3 (Alcoa CS 400), AlN (HCST Grade C) and Y_2O_3 (HCST Grade C) were attrition milled in isopropanol for a period of 4 h at 700 rpm, using polyamide milling vials and stirrers and Si_3N_4 milling media. After attrition milling, the slurries were separated from the milling media and also possible wear debris by screening. Drying was performed by rotational evaporation and subsequent holding at 65°C in a drying chamber for 48 h. The resulting agglomerates were subsequently dry sieved with a mesh size of 160 μm. The granulated powders had a good flowability and were pressed isostatically at pressures of 240–600 MPa.

The green bodies were densified in graphite-heated gas pressure furnaces (KCE GmbH, Germany, and Thermal Technology Inc., USA) at N_2 pressures up to 10 MPa. Table 1 gives an example of the sintering programs used. The results reported here are for materials with additive contents of 10 vol.%, additive compositions of 60 AlN : 40 Y_2O_3 and 80 AlN : 20 Y_2O_3 (mol%), and SiC compositions of 100 α : 0 β and 10 α : 90 β. These materials are labeled as 60α, 80α, 60β and 80β, regardless of the phases present in the sintered samples. The sintering temperatures necessary for complete densification were found by increasing the plateau temperature T_S stepwise, so that the relative density determined by Archimedes' method was at least 99.3%. All samples were characterised for mass loss during sintering. Strictly speaking, the relative density values are distorted by reactions between SiC and additives and by mass loss, since theoretical densities were calculated from the densities of the starting substances by the rule of mixtures.

By pressureless sintering, fully dense samples can be obtained. However, applying an increased nitrogen pressure of 0.2 MPa is useful for suppressing gas phase reactions and decreasing the mass loss during sintering from about 7 to 2.5%. This corresponds to the oxygen present in form of a SiO_2 layer on the surface of the SiC powder particles. The sintering step under a pressure of 10 MPa, which can be added after pore closure, yields somewhat higher strength values as a result of isostatic-pressure assisted densification.[3] For the materials 60β and 80β, an additional annealing time at 1950°C was

Table 1
Sintering and annealing programs for complete densification and microstructure evolution of LPS–SiC materials

Nomenclature	SiC	Additives	Sintering program		
	(90 vol.%)	(10 vol.%)	Ramp	Atmosphere	Holding Time
			20°C→1000°C, 20 K/min	vacuum	
			1000→1600°C, 20 K/min	0.2 MPa N_2	30 min
			1600°C→T_{max}, 10 K/min	0.2 MPa N_2	30 min
				10 MPa N_2	30 min
			T_{max}→1950°C, 20 K/min	0.2 MPa N_2	t_{ann}
			1950°C→20°C, 50 K/min	0.2 MPa N_2	
60α	100 α	60 AlN/ 40 Y_2O_3	T_{sinter} = 1950°C		t_{ann} = 0 h
60β	90 β/ 10 α	60 AlN/ 40 Y_2O_3	T_{sinter} = 1970°C		t_{ann} = 8…16 h
80α	100 α	80 AlN/ 20 Y_2O_3	T_{sinter} = 1960°C		t_{ann} = 0 h
80β	90 β/ 10 α	80 AlN/ 20 Y_2O_3	T_{sinter} = 1980°C		t_{ann} = 16 h

added to complete the phase transformation from β-SiC to α-SiC. The mass loss of samples annealed for 16 h was about 4.5%.

Crystallographic phases and microstructures were monitored by X-ray powder diffraction (XRD) using monochromatic CuK_α radiation and a position sensitive detector spanning a 2Θ angle of 8°. Ceramographic sample preparation included a final polishing step with 1 μm diamond suspension, and plasma etching in an equimolar mixture of CF_4 and O_2. A scanning electron microscope (SEM) with thermal field emission cathode (Zeiss DSM 982) was utilised for microstructural characterisation. The acceleration voltage was reduced to 3–5 keV to avoid charging effects. The energy dispersive microanalysis (EDX) spectrometer attached to the microscope allows the light elements, N and O, to be analysed semi-quantitatively. Grain sizes and aspect ratios were determined by using an image analysis software (Imtronic Image C).

Four-point bending strengths (σ^{4pt}) were determined using a fixture with inner and outer spans of 7 and 20 mm. For each material, at least 6 specimens were tested. Samples with dimensions of 3×4×25 mm^3 were cut from larger sintered bars by means of a diamond saw. After grinding on all sides, the tensile surfaces were polished to a 1 μm finish and the tensile edges were bevelled. The samples were loaded with a constant cross head speed of 5 mm/s at room temperature or 0.1 mm/min at temperatures between 1000 and 1500°C. High temperature testing was performed in air, after a dwell time of 10 min at the testing temperature.

Fracture toughness at ambient temperature was determined with the indentation crack length method (K_{Ic}^{ICL}). After polishing to a 1 μ finish, at least 10 Vickers indentations per specimen were introduced with a load of 100 N and loading times of 15 s. The fracture toughness was calculated from the lengths of edge cracks and indentation diagonals using a formula valid for semi-circular crack systems.[9] Young's moduli were measured by the pulse-echo method. For the K_{Ic} calculations, values of 390 GPa for the materials 60β and 80β and 420 GPa for the materials 60α and 80α were used. The high-temperature fracture toughness was measured, at crack tip temperatures of 550–1050°C, using the thermal stress method (K_{Ic}^{TS}) of Schneider et al.[10] This involves selective heating of the center of a notched disc (12 mm Ø×0.3 mm, surfaces polished to 1 μm finish) by means of a halogen reflector lamp in order to generate a temperature gradient. The tangential stress field, which is generated due to the temperature gradient, causes crack initiation and growth at the notch root. During stationary heating, the crack propagation is stable after a short initial period and can be monitored with a long-distance microscope. From the crack length as a function of the thermally induced stress distribution, K_{Ic}^{TS} is calculated.

3. Results and discussion

Samples 60α [Fig. 1(a)] and 80α, which are produced from pure α-SiC powder, exhibit fine-grained and equiaxed microstructures. By quantitative image analysis, average grain sizes of 1.0 and 0.4 μm were found, respectively. In materials obtained from mixtures of 90% β-SiC and 10% α-SiC, platelet microstructures develop during post-densification heat treatments [Fig. 1(b)]. Anisotropic grain growth occurs during the β→α transformation which is completed after 8 h (60β) or 16 h (80β) at 1950°C. The aspect ratio of the platelets tends to decrease again if the annealing time is extended beyond the completion of the phase transformation. After 16 h at 1950 °C, mean platelet diameters of 2.2 and 2.0 μm and aspect ratios of 3.7 : 1 and 2.9 : 1 were measured for 60β and 80β, respectively [8]. When the density of the α-SiC nuclei in the starting powder is decreased, higher aspect ratios can be obtained, e. g. up to 8 : 1 at a β-SiC to α-SiC ratio of 99 : 1.[11] In materials based on pure α-SiC, in contrast, platelet formation is suppressed even for long annealing times because steric

hindrance occurs from the very beginning of grain growth. Apart from the influence of seeding, the kinetics of phase transformation and grain growth are slowed down at higher nitrogen content of the intergranular phase. The viscosity of silicate melts is known to increase at increased nitrogen content,[12,13] impeding the transport of matter through the melt. The higher densification temperature of the 80AlN materials is also attributed to this behaviour (Fig. 2).

In Fig. 1, areas of different etching by the fluorine-containing plasma are clearly discernible within many of the SiC grains. This *core-rim* structure [15] is indicative of the solution/precipitation sintering mechanism, the undissolved *core* regions containing less dopant atoms (Al, N) and being etched to a larger extent by the fluorine plasma than the *rim* regions of re-precipitated α-SiC.

The influence of anisotropic grain growth on the fracture toughness K_{Ic}^{ICL} is shown in Fig. 3. There is a steady increase of K_{Ic}^{ICL} with increasing annealing time (1925°C, N_2 atmosphere). In the case of 60β, K_{Ic}^{ICL} remains constant at a value of 6 MPa$\sqrt{m}$ when the annealing time is extended beyond the completion of the β→α transformation (not shown here). The fracture toughness of samples produced from pure α-SiC does not change significantly upon annealing.

The mechanisms that are responsible for the increased K_{Ic} can be identified by SEM examination of crack paths.[12] At room temperature, crack deflection, elastic bridging, mechanical interlocking and platelet fracture were identified as the energy dissipating processes in the crack wake, while platelet pull-out was encountered only occasionally. In K_{Ic}^{TS} samples fractured at high temperature, pull-out was observed frequently, which can be explained by the softening of the intergranular glass phase at elevated temperatures. This is accompanied by a further increase of K_{Ic}^{TS} (up to a value of 8

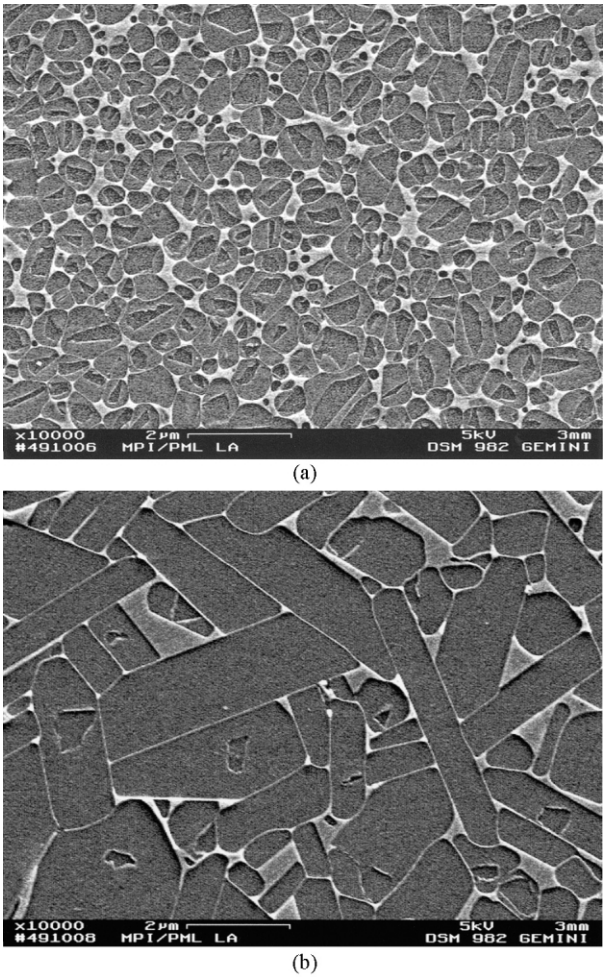

Fig. 1. SEM micrographs of (a) LPS–SiC 60α, as-sintered, and (b) LPS–SiC 60β, annealed (1950°C/16h).

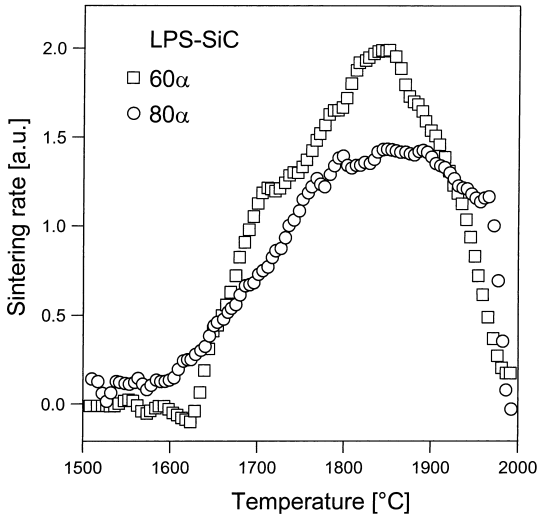

Fig. 2. Densification rates as a function of the nitrogen content of the sintering additive (heating rate: 10 K/min, atmosphere: 0.1 MPa N_2).

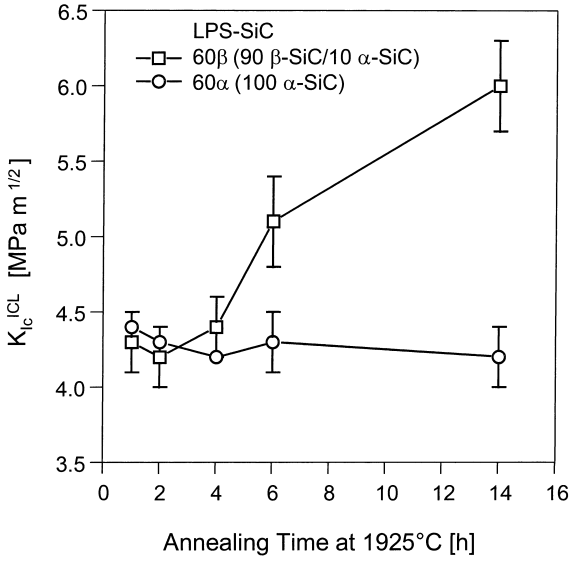

Fig. 3. Fracture toughness of ceramics based on α-SiC (60α) and β-/α-SiC mixtures (60β), as a function of the annealing time.

MPa$\sqrt{m}$ — cf. Table 2). In the more globular microstructure of the α-SiC derived materials, a limited amount of crack bridging was also detected.

Furthermore, in K_{Ic}^{TS} samples based on pure α-SiC and tested in air, partial filling of the crack wake with an oxidic glass phase was observed, which consists of $\geqslant$90 wt.% SiO_2 according to EDX analyses (Fig. 4). The oxidation product exhibits a low viscosity at the reaction temperature and is able to fill the crack wake over distances up to 50 μm. In polished samples oxidised for times ranging from 12 to 6000 min at 1200°C, the formation of continuous oxide films with thicknesses between 0.44 and 2.0 μm was observed (Fig. 5). As a consequence of the crack healing (or shortening), the crack growth exponent during sub-critical crack growth in air was found to be increased compared to that in argon atmosphere: $n_{air} = 76.5$ vs. $n_{Ar} = 35.5$ in the material 80α at crack tip temperatures between 1040 and 1060°C. In platelet microstructures, no crack healing is detectable except sporadic viscous bridges. Accordingly, n_{air} of 80β is smaller than that of 80α (Fig. 6). A probable explanation for this behaviour is that the nitrogen content of the grain boundary phases is lower in the high-temperature annealed platelet materials than in the as-sintered fine-grained materials due to preferential thermal decomposition of the nitrogen-containing phases. This limits the opportunities for additional oxidation of the grain boundary film.

Table 2
Fracture toughness of LPS–SiC

Material	K_{Ic}^{ICL} [MPa$\sqrt{m}$]		K_{Ic}^{TS} (MPa$\sqrt{m}$]	
	As-sintered	1950°C/16 h	As-sintered	1950°C/16 h
60α	4.4±0.2		4.6±0.5	
60β	4.9±0.2	6.2±0.3	n. a.	7.5±0.6
80α	4.3±0.2		4.0±0.4	
80β	3.9±0.3	6.3±0.2	n.a.	8.0±0.5

For the as-sintered materials 60α and 80α, room temperature bending strengths of 607±80 MPa and 436±136 MPa were measured, respectively. For 60β and 80β, after a heat treatment of 16 h at 1950°C/0.2 MPa N_2, the corresponding values were determined to be 551±146 MPa and 487±92 MPa. In Fig. 7, the strength behaviour is shown as a function of temperature. Samples 60β and 80β exhibit constant strength values from room temperature to 1000°C. Between 1200 and 1400°C, the intergranular phase undergoes softening which results in a decrease of σ^{4pt}. In contrast, the decrease of σ^{4pt} is preceded by strength maxima at temperatures between 1000 and 1200°C in the fine-grained materials 80α and 60α. It seems reasonable to suppose that this effect is related to the crack healing that is observed in these materials.

In order to investigate whether the oxidation-induced strength enhancement can be maintained down to ambient temperature, isothermal heat treatments were conducted at 1200°C in air. The resulting room temperature

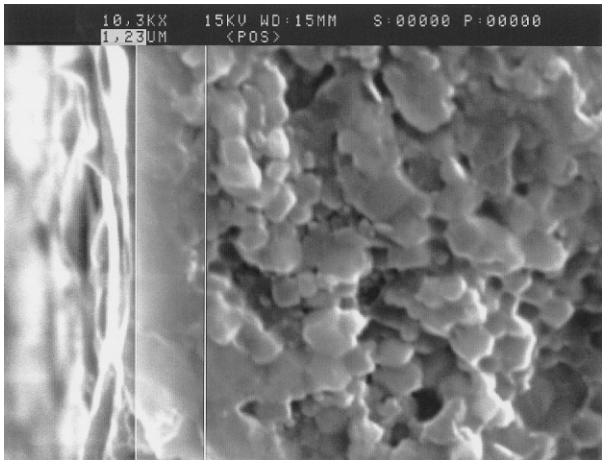

Fig. 5. Formation of an oxide film on the surface of LPS–SiC 80α (1200°C/600 min in air).

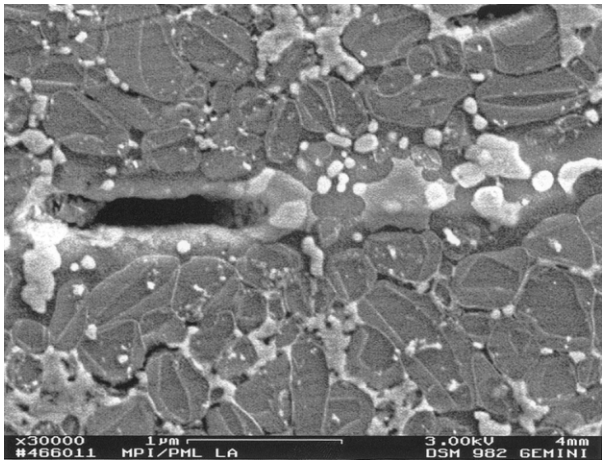

Fig. 4. Crack healing in fine-grained LPS–SiC 60α (K_{Ic}^{TS} sample).

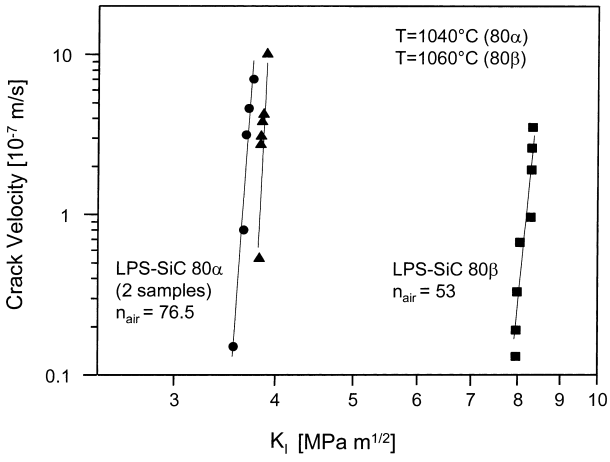

Fig. 6. Sub-critical crack growth in LPS–SiC 80α and 80β (in air).

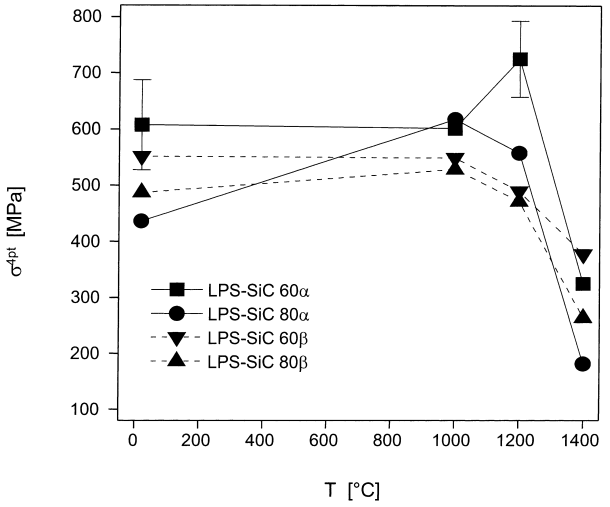

Fig. 7. Temperature-dependent bending strength of fine-grained and platelet-strengthened LPS–SiC materials (in air).

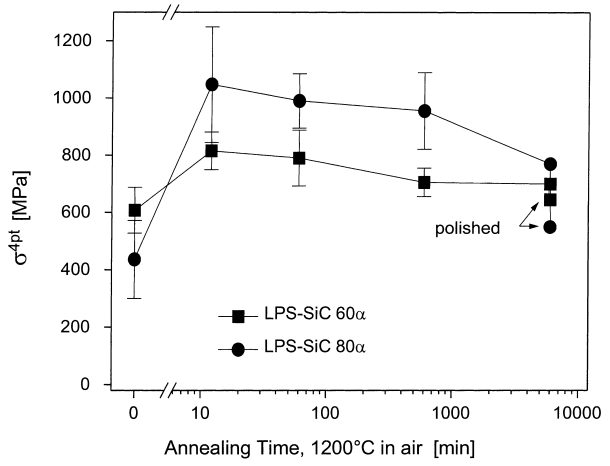

Fig. 8. Strength behaviour upon surface oxidation; for the annealing time of 100 h, the residual strength after re-polishing is also indicated.

strengths were markedly higher than those of unoxidised samples (Fig. 8). After an annealing time of 12 min, average strength values of 1047±202 MPa (80α) and 815±66 MPa (60α) were measured. Upon continuing oxidation, σ^{4pt} decreases again, but the residual strength after 6000 min is still higher than the starting value. Removal of a surface layer several μm thick by polishing cancels the strength increase only to some extent; the residual strengths after oxidation for 12 min are still 938±103 MPa (80α) and 783±68 MPa (60α).

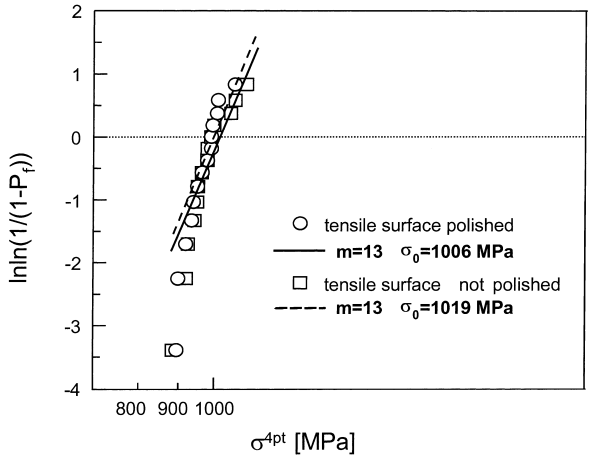

Fig. 9. Weibull diagram for fine-grained bending samples after surface oxidation.

This is a remarkable finding because the removed layer is cetainly thicker than the crack-healing oxide film (cf. Fig. 5). The Weibull modulus, which can be extracted from a plot of failure probability against bending stress (Fig. 9), and which represents a criterion for the reliability of ceramic parts, increases from $m=7$ to $m=13$ in surface-oxidised LPS-SiC 80α. This high value is also retained upon re-polishing oxidised samples.

Finally, there is also an increase in the indentation fracture toughness of oxidised 80α samples (Table 3), the penetration depth of the Vickers diamond (≈ 50 μm) again being several times larger than the thickness of the oxide film of Fig. 5. Therefore, the observed oxide film cannot be the decisive factor for the increased K_{Ic}^{ICL}, i. e. a second strengthening mechanism is likely to be operative in addition to the filling of surface flaws by the glass phase.

It had been shown earlier,[16] that the creation of compressive stresses in the surface layer of brittle materials is accompanied by an apparent increase in the fracture toughness of the surface layer. In the present materials, the following sequence of phase transformations from oxynitridic to oxidic secondary phases is detected by XRD as a result of the heat treatments in air:[4]

$$Y_{10}Al_2Si_3O_{18}N_4 \rightarrow Y_2AlSi_2O_7N_2$$

$$\rightarrow Al_5Y_3O_{12} + Y_2Si_2O_7$$

Similar oxidation processes may be assumed for the amorphous fraction of the intergranular phase. In the

Table 3
Fracture toughness as a function of annealing time in air, LPS–SiC 80α

Annealing time (1200°C in air) [min]	0	12	60	600	6000
K_{Ic}^{ICL} oxidised [MPa$\sqrt{m}$]	4.3±0.2	6.1±0.2	5.7±0.3	5.4±0.2	4.8±0.3
K_{Ic}^{ICL} polished [MPa$\sqrt{m}$]		5.6±0.3	5.2±0.1	5.0±0.1	4.4±0.4

presence of amorphous surface layers, the oxidation rate of SiC at 1300°C is known to increase by a factor of 30 or more.[17] The extremely fast oxygen transport through the amorphous phase thus allows selective oxidation to take place in a relatively thick surface layer. The penetration depth of the CuK_α radiation is about 20 μm.

Upon oxidation, the average density of both crystalline and amorphous oxynitrides tends to decrease owing to the decreasing number of bonds per anion.[14] For example, the densities of $Y_2Si_2O_7$ (4.03 g cm^{-3}) and YAG (4.55 g cm^{-3}) are lower than that of $Y_{10}Al_2Si_3O_{18}N_4$ (4.68 g cm^{-3}). This volume gain of the intergranular phase is likely to induce large compressive stresses which can remove surface flaws, leading to an effective strengthening of the surface. By comparison with the layer thicknesses probed by XRD (20 μm) and Vickers indentations (50 μm), the extension of the stress states into the bulk can be estimated. Upon further oxidation, the bending strength deteriorates due to damaging of the SiC base material. The fact that no high-temperature strengthening effect is observed in platelet materials, is explained by the preferential loss of nitrogen from the additive during the extended heat treatments at 1950°C which are required for anisotropic grain growth. Further investigations, aiming at the evaluation of stress states by XRD as well as nitrogen concentration profiles by resonant nuclear reaction analysis (RNRA), are currently being performed.[18]

4. Conclusions

Fully dense SiC ceramics can be obtained by liquid phase sintering with AlN–Y_2O_3 additives, without the necessity of a powder bed. In view of the thermal decomposition of AlN, sintering is advantageously performed in a moderate nitrogen overpressure. The materials obtained have a good potential for microstructure design by anisotropic grain growth of α-SiC. In platelet-strengthened materials, high-temperature toughness values of $K_{Ic}^{TS} = 8$ MPa$\sqrt{}$m can be achieved.

The high temperature bending strength of a fine-grained variant of the present LPS–SiC is characterised by a strength maximum around 1200°C. This effect is believed to be due to the generation of compressive stress by the selective oxidation of intergranular oxynitride phases. By annealing at 1200°C in air, it is possible to achieve a four-point bending strength of about 1 GPa at room temperature with simultaneous doubling of the Weibull modulus. In other words, the ambient strength of the material is largely determined by surface flaws, whereas the bulk microstructure is sufficiently defect-free to allow an outstanding strength level to be reached.

Compressive stress states in a surface layer due to oxidation, nitridation or the application of coatings are known to cause surface strengthening in ceramics.[18–21] However, the magnitude of the present selective oxidation phenomenon, the significant thickness of the influenced layer and the ease with which the heat treatment is performed, seem to generate a particularly high potential for applications in enhancing the reliability of LPS–SiC parts.

Acknowledgements

This work was funded in part by the federal state of Baden-Württemberg (Keramikverbund Karlsruhe-Stuttgart). The authors are thankful to the technical staff of PML Stuttgart for assisting with the experimental work and to M. Rozumek for carefully reading the manuscript.

References

1. Hoffmann, M. J. In *Tailoring of Mechanical Properties of Si_3N_4 Ceramics*, ed M. J. Hoffmann and G. Petzow. Kluwer Academic, Dordrecht, 1994, p. 59.
2. Padture, N. P. J., *Am. Ceram. Soc.*, 1994, **77**, 519.
3. Nader, M. Doctoral thesis, University of Stuttgart, 1995.
4. Wiedmann, I. Doctoral thesis, University of Stuttgart, 1998.
5. Mulla, M. A. and Krstic, D., *J. Mater. Sci.*, 1994, **29**, 934.
6. Wiedmann, I., Nader, M., Hoffmann, M. J. and Aldinger, F. In *Werkstoffwoche 1996, Symp. 7: Materialwiss. Grundlagen*, ed. F. Aldinger and H. Mughrabi. DGM Informationsges, Oberursel, 1997, p. 515.
7. Seifert, H. J., Lukas, H. L. and Petzow, G. In *Design Fundamentals of High Temperature Composites, Intermetallics, and Metal-Ceramics Systems*, ed. R. Y. Lin et al. Min., Met. Mater. Soc., Warrendale, 1995, p. 297.
8. Chia, K. Y., Boecker, W. D. G. and Storm, R. S. US Patent. 5,298,470,1994.
9. Anstis, G. R. P., Chantikul, P., Lawn, B. R. and Marshall, D. B., *J. Am. Ceram. Soc.*, 1981, **64**, 533.
10. Schneider, G. A. and Petzow, G., *J. Am. Ceram. Soc.*, 1991, **74**, 98.
11. Schneider, G. A., Magerl, F., Hahn, I. and Petzow, G. In: *Thermal Shock and Thermal Fatigue Behaviour of Advanced Ceramics*, ed. G. A. Schneider and G. Petzow. Kluwer Academic, Dordrecht, 1993.
12. Keppeler, M., Reichert, H.-G., Broadley, J. M., Thurn, G., Wiedmann, I. and Aldinger, F., *J. Eur. Ceram. Soc.*, 1998, **18**, 521.
13. Drew, R. A. L., Hampshire, S. and Jack, K. H. In *Progress in Nitrogen Ceramics*, ed. F. L. Riley. Martinus Nijhoff, Boston, 1983, p. 323.
14. Hampshire, S., Nestor, E., Flynn, R., Besson, J.-L., Rouxel, T., Lemercier, H., Goursat, P., Sebai, M., Thompson, D. P. and Liddell, K., *J. Eur. Ceram. Soc.*, 1994, **14**, 261.
15. Sigl, L. S. and Kleebe, H.-J. J., *Am. Ceram. Soc.*, 1993, **76**, 773.
16. Gruninger, M. F., Lawn, B. R., Farabough, E. N. and Wachtman, J. B., *J. Am. Ceram. Soc.*, 1987, **70**, 344.
17. Ogbuji, L. U. J. T., *J. Am. Ceram. Soc.*, 1997, **80**, 1544.
18. Schneider, J. A., Rixecker, G. and Aldinger, F. to be published.
19. Choi, S. R. and Tikare, V., *Script Metall.*, 1992, **26**, 1263.
20. Jiang, D. L., She, J. H., Tan, S. H. and Greil, P., *J. Am. Ceram. Soc.*, 1992, **75**, 2586.
21. Lakshmiarayanan, R., Shetty, D. K. and Cutler, R. A., *J. Am. Ceram. Soc.*, 1996, **79**, 79.